New Hydride-Containing Mixed-Metal–Gold Phosphine Clusters. Crystal Structures of $[Pt(H)(CuCl)(AuPPh_3)_8](NO_3)$ and $[Pt(H)(CuCl)_2(AuPPh_3)_8](NO_3)$

T. G. M. M. Kappen, P. P. J. Schlebos, J. J. Bour, W. P. Bosman, J. M. M. Smits, P. T. Beurskens, and J. J. Steggerda*

Department of Inorganic Chemistry and Crystallography, Faculty of Science, University of Nijmegen, Toernooiveld, 6525 ED Nijmegen, The Netherlands

Received August 25, 1994[⊗]

Reactions of $[Pt(AuPPh_3)_8](NO_3)_2$ with M(I) species (M = Cu, Au) under H_2-atmosphere yield several new hydride-containing mixed-metal–gold phosphine cluster compounds. Two new hydride-containing PtAuCu clusters are obtained in this way: $[Pt(H)(CuCl)(AuPPh_3)_8](NO_3)$ (**1**) and $[Pt(H)(CuCl)_2(AuPPh_3)_8](NO_3)$ (**2**). Considerations on the solvent dependency show that the Brønsted acidity of the solvent used is crucial in controlling the formation of **1** or **2**. Clusters **1** and **2** were characterized by elemental analyses, ICP analyses, and IR and NMR (^{31}P and ^{195}Pt) spectroscopy; their crystal and molecular structures have been determined by single-crystal X-ray analyses. Compound **1** crystallizes in the monoclinic space group $P2_1$, with $Z = 2$, $a = 15.284(8)$ Å, $b = 26.004(2)$ Å, $c = 16.558(2)$ Å, $\beta = 95.27(5)°$, and $V = 6636$ Å^3; Mo Kα radiation was used. The residuals are $R = 0.083$ and $wR_2 = 0.18$ for 10 495 observed reflections and 372 variables. **2** crystallizes in the triclinic space group $P\bar{1}$, with $Z = 2$, $a = 15.349(4)$ Å, $b = 16.949(2)$ Å, $c = 29.037(7)$ Å, $\alpha = 78.95(1)°$, $\beta = 74.87(2)°$, $\gamma = 84.74(2)°$, and $V = 7150$ Å^3; Mo Kα radiation was used. The residuals are $R = 0.085$ and $wR_2 = 0.22$ for 15308 observed reflections and 773 variables. Both clusters have a central platinum atom surrounded by eight gold atoms and one (for **1**) or two (for **2**) copper atoms; the gold atoms are attached to triphenylphosphine ligands, whereas the copper atoms are attached to chloride ligands. The crystal structures of **1** and **2** show that the copper atoms in these clusters are located "trans" to the hydride ligand. $[Pt(H)(PPh_3)(CuCl)(AuPPh_3)_6]^+$ (**5**) is obtained from the reaction of the cluster $[Pt(H)(PPh_3)(AuPPh_3)_7](NO_3)_2$ with $[PPh_3CuCl]_4$. **5** was characterized by IR, ^1H NMR, ^{31}P NMR and ^{195}Pt NMR spectroscopy and by FAB-MS. In addition to these PtAuCu clusters this paper also reports several new $PtHAu_9$ cluster compounds: $[Pt(H)(AuPy)(AuPPh_3)_8](NO_3)_2$ (**3**) (in which Py = C_5H_4N), $[Pt(H)(AuCl)(AuPPh_3)_8](NO_3)$ (**4a**), $[Pt(H)(AuBr)(AuPPh_3)_8](Br)$ (**4b**), and $[Pt(H)(AuSCN)(AuPPh_3)_8](SCN)$ (**4c**). The pyridine ligand of **3** can be substituted easily by Cl^-, Br^- or SCN^- to give **4a**, **4b**, or **4c**, respectively. The thiocyanate ligand of **4c** is shown to be sulfur-coordinated to a gold atom.

Introduction

Recent studies on mixed-metal–gold clusters have shown that the geometry of these clusters is related to their electron configuration:[1] toroidal geometries are observed for $(S^\sigma)^2(P^\sigma)^4$ (16 electron) clusters, whereas $(S^\sigma)^2(P^\sigma)^6$ (18 electron) cluster compounds adopt spheroidal geometries. The reactivities of such cluster compounds can also be rationalized in terms of these electron configurations. Nucleophilic addition reactions of a two-electron donating group to the centers of toroidal $(S^\sigma)^2(P^\sigma)^4$ clusters have been reported to result in $(S^\sigma)^2(P^\sigma)^6$ clusters with spheroidal geometries.[2-4]

Electrophilic additions on the other hand have been observed for $(S^\sigma)^2(P^\sigma)^4$ clusters as well as for $(S^\sigma)^2(P^\sigma)^6$ clusters:[5-7] The electron configuration and the accompanying geometry classification of the cluster are not changed by such electrophilic additions. Oxidative additions to $(S^\sigma)^2(P^\sigma)^4$ clusters, to yield $(S^\sigma)^2(P^\sigma)^6$, are particularly interesting.[8] The oxidative addition of H_2 to $[Pt(AuPPh_3)_8]^{2+}$ is fast and fully reversible at ambient pressures and temperatures, and results in the formation of an $(S^\sigma)^2(P^\sigma)^6$ dihydride cluster:[9]

$$[Pt(AuPPh_3)_8]^{2+} + H_2 \rightleftarrows [Pt(H)_2(AuPPh_3)_8]^{2+}$$

This oxidative addition reaction plays a crucial role in the formation of the compounds $[Pt(H)(AgNO_3)(AuPPh_3)_8](NO_3)$ and $[Pt(H)(AgNO_3)_2(AuPPh_3)_8](NO_3)$:[10] the $(S^\sigma)^2(P^\sigma)^6$ dihydride gives rise to these new compounds through electrophilic substitution and electrophilic addition reactions of Ag(I) units.

In this paper we report the analogous reactions with CuCl and $AuPPh_3X$. Two new hydride containing PtAuCu clusters were obtained in this way: $[Pt(H)(CuCl)(AuPPh_3)_8](NO_3)$ (**1**) and $[Pt(H)(CuCl)_2(AuPPh_3)_8](NO_3)$ (**2**). The hydride containing $[Pt(H)(AuPy)(AuPPh_3)_8](NO_3)_2$ (**3**) (in which Py = C_5H_4N) was

[⊗] Abstract published in *Advance ACS Abstracts,* March 15, 1995.

(1) Kanters, R. P. F.; Steggerda, J. J. *J. Cluster Sci.* **1990**, *1*, 229.
(2) Kanters, R. P. F.; Schlebos, P. P. J.; Bour, J. J.; Bosman, W. P.; Behm, H. J.; Steggerda, J. J. *Inorg. Chem.* **1988**, *27*, 4034.
(3) Van der Velden, J. W. A.; Bour, J. J.; Bosman, W. P.; Noordik, J. H. *Inorg. Chem.* **1983**, *22*, 1913.
(4) Kanters, R. P. F.; Schlebos, P. P. J.; Bour, J. J.; Wijnhoven, J.; van den Berg, E.; Steggerda, J. J. *J. Organomet. Chem.* **1990**, *388*, 233.
(5) Schoondergang, M. F. J.; Bour, J. J. Schlebos, P. P. J.; Vermeer, A. W. P.; Bosman, W. P.; Smits, J. M. M.; Beurskens, P. T.; Steggerda, J. J. *Inorg. Chem.* **1991**, *30*, 4704.
(6) Kanters, R. P. F.; Schlebos, P. P. J.; Bour, J. J.; Bosman, W. P.; Smits, J. M. M.; Beurskens, P. T.; Steggerda, J. J. *Inorg. Chem.* **1990**, *29*, 324.
(7) Kappen, T. G. M. M.; van den Broek, A. C. M.; Schlebos, P. P. J.; Bour, J. J.; Bosman, W. P.; Smits, J. M. M.; Beurskens, P. T.; Steggerda, J. J. *Inorg. Chem.* **1992**, *31*, 4075.
(8) Bour, J. J.; van den Berg, W.; Schlebos, P. P. J.; Kanters, P. P. J.; Schoondergang, M. F. J.; Bosman, W. P.; Smits, J. M. M.; Beurskens, P. T.; Steggerda, J. J.; van der Sluis, P. *Inorg. Chem.* **1990**, *29*, 2971.
(9) Kappen, T. G. M. M.; Bour, J. J.; Schlebos, P. P. J.; Roelofsen, A. M.; van der Linden, J. G. M.; Steggerda, J. J.; Aubart, M. A.; Krogstadt, D. A.; Schoondergang, M. F. J.; Pignolet, L. H. *Inorg. Chem.* **1993**, *32*, 1074.
(10) Kappen, T. G. M. M.; Schlebos, P. P. J.; Bour, J. J.; Bosman, W. P.; Beurskens, G.; Smits, J. M. M.; Beurskens, P. T.; Steggerda, J. J. To be submitted for publication.

0020-1669/95/1334-2133$09.00/0

obtained from the reaction of $[Pt(AuPPh_3)_8](NO_3)_2$ with $AuPPh_3NO_3$ in pyridine solution under H_2-atmosphere. The Py ligand was easily substituted by Cl^-, Br^-, or SCN^- to give $[Pt(H)(AuX)(AuPPh_3)_8]^+$ (**4**) (in which X = Cl, Br or SCN, respectively). We also report the formation of another hydride-containing PtAuCu cluster, $[Pt(H)(PPh_3)(CuCl)(AuPPh_3)_6]^+$ (**5**), obtained from the reaction of $[Pt(H)(PPh_3)(AuPPh_3)_7](NO_3)_2$ with $[PPh_3CuCl]_4$. All newly reported compounds **1**−**5** are $(S^\sigma)^2(P^\sigma)^6$ clusters.

Experimental Section

Measurements. Elemental C, H, and N analyses were carried out at the microanalytical department of the University of Nijmegen. ICP analyses of the copper-containing clusters, giving Pt:Au:Cu ratios were carried out on a Plasma 200 ICP-AE spectrometer in DMSO solutions of the cluster compounds with $[Pt(CO)(CuCl)(AuPPh_3)_8](NO_3)_2$[5] and $[Pt(CO)(CuCl)_2(AuPPh_3)_7](NO_3)$[5] used for calibration. Due to partial overlap of the spectral emission lines of copper with those used for phosphorus detection, determination of the phosphorus content was not performed for the copper containing cluster compounds. The ICP analyses of PtAu cluster compounds without copper were obtained from DMSO solutions of the compounds on the aforementioned spectrometer providing Pt:Au:P ratios with $[Pt(AuPPh_3)_8](NO_3)_2$[11] used for calibration.

Fast atom bombardment mass spectroscopy (FAB-MS) on **5** was performed by the mass spectrometry service laboratory of the University of Minnesota on a VG Analytical Ltd. 7070E-HF mass spectrometer. The FAB-MS spectrum was taken from a nitromethane solution of the compound under inert atmosphere by means of continuous-flow conditions to prevent exposure of the compound to air. CsI was used as the standard for mass-calibration; further experimental details are given elsewhere.[12]

$^{31}P\{^1H\}$ NMR spectra of CH_2Cl_2 solutions of the cluster compounds were recorded on a Bruker WM-200 spectrometer, operating at 81.015 MHz, and on a Bruker AM-500 spectrometer, operating at 202.462 MHz, with trimethylphosphate (TMP) in CD_2Cl_2 as external reference; ^1H NMR spectra were recorded in CD_2Cl_2 solutions (for compound **3**) or in $CDCl_3$ solutions (for compound **5**) on a Bruker AM-500 spectrometer operating at 500.13 MHz with tetramethylsilane (TMS) as reference. The ^{195}Pt NMR spectra were recorded at 43.02 MHz on the above-mentioned Bruker WM-200 spectrometer using $CDCl_3$ solutions of **5** and CD_2Cl_2 solutions for all other cluster compounds; K_2PtCl_6 in D_2O was used as external reference. Phosphorus decoupling during ^{195}Pt NMR experiments was performed with a PTS 200 synthesizer. ^2H NMR experiments were run on a Bruker WM-200 spectrometer (at 30.722 MHz) and on a Bruker AM-500 spectrometer (at 76.774 MHz) in CH_2Cl_2 solutions. The infrared (IR) spectra were measured in CsI pellets on a Perkin-Elmer 1720-X Fourier transform infrared spectrometer in the range from 4000 to 220 cm^{-1}.

Preparations. $AuPPh_3NO_3$,[13] $AuPPh_3Cl$,[14] CuCl,[15] and $[PPh_3CuX]_4$ (X = Cl, Br, I)[16] were prepared according to literature methods. This is also the case for the cluster compounds $[Pt(AuPPh_3)_8](NO_3)_2$,[11] $[Pt(CuCl)(AuPPh_3)_8](NO_3)_2$,[5] and $[Pt(H)(PPh_3)(AuPPh_3)_7](NO_3)_2$.[17] All solvents were of reagent grade and were used without further purification, except for those used in the synthesis and characterization of $[Pt(H)(PPh_3)(CuCl)(AuPPh_3)_6]^+$ (**5**), which were purified according to literature methods.

$[Pt(H)(CuCl)(AuPPh_3)_8](NO_3)$ (1). A 100-mg (0.025-mmol) sample of $[Pt(AuPPh_3)_8](NO_3)_2$ was dissolved in 4 mL of acetone. Dihydrogen was bubbled through this brown solution for 10 min upon which the color changed to red-brown. To this solution was then added 2.7 mg (0.027 mmol) of CuCl under dihydrogen atmosphere, which further changed the color to deep red. After 30 min of stirring, an orange-red precipitate was formed and the reaction mixture was stirred for 5 h more; the dihydrogen atmosphere was then replaced by air and the orange-red precipitate was filtered off and washed with 2 mL of acetone and finally twice with 10 mL of diethyl ether. Red crystals of $[Pt(H)(CuCl)(AuPPh_3)_8](NO_3)$ (**1**) were obtained by slow diffusion of diethyl ether into a 1:1 (v/v) dichloromethane−methanol solution of the sample (yield: 81 mg, 0.020 mmol; 80%, calculated for Pt).

Anal. Calcd for $PtAu_8CuP_8C_{144}H_{121}NO_3Cl$ (mol wt 4031.15): C, 42.91; H, 3.03; N, 0.35. Found: C, 42.35; H, 3.08; N, 0.33. ICP: Pt:Au:Cu = 1:8.1:1.0. IR: uncoordinated NO_3 showed a broad band at 1359 cm^{-1} in addition to several absorption bands originating from the PPh_3 ligands. ^{31}P NMR: δ = 54.1 ppm with $^2J(P-^{195}Pt)$ (doublet) = 410 Hz. ^{195}Pt NMR: δ = −6015 ppm with $^1J(Pt-^1H)$ (doublet) = 678 Hz and $^2J(Pt-^{31}P)$ (nonet) = 410 Hz.

$[Pt(H)(CuCl)_2(AuPPh_3)_8](NO_3)$ (2). (A) A 70-mg (0.018-mmol) sample of $[Pt(AuPPh_3)_8](NO_3)_2$ was dissolved in 3 mL of acetone. After dihydrogen was bubbled through this solution for 10 min, which changed the color from brown to red-brown, 4.0 mg (0.040 mmol) of CuCl was added under dihydrogen atmosphere. This changed the color of the mixture to deep red, and after 30 min of stirring an orange-red precipitate was obtained. The reaction mixture was stirred for 1 day more; the reaction vessel was then opened to air, and the orange-red precipitate was filtered off and subsequently washed with acetone and diethyl ether. ^{31}P NMR characterization of this precipitate revealed the presence of **2** in ca. 60% yield.

The same orange-red precipitate could be obtained from the analogous reaction in methanol. However, when this reaction was performed in dichloromethane the reaction mixture had to be evaporated to dryness after reacting for 1 day to obtain the same product.

(B) Dihydrogen was bubbled through a solution of $[Pt(CuCl)(AuPPh_3)_8](NO_3)_2$ (70 mg, 0.017 mmol) in 10 mL of methanol (or dichloromethane) for 15 min after which this solution was stirred under dihydrogen atmosphere for 2 h. This changed the color of the solution from brown to red. After this reaction period, the dihydrogen atmosphere was replaced by air, upon which the color changed to brown-red, and the reaction mixture was evaporated to dryness under reduced pressure. ^{31}P NMR characterization of a dichloromethane solution of the resulting powder only revealed the presence of **2** and $[Pt(AuPPh_3)_8]^{2+}$ in equal amounts.

Monitoring this reaction with ^{31}P NMR spectroscopy revealed the intermediate presence of **1** during the early stages of this reaction (see Results and Discussion).

(C) A 70-mg (0.018-mmol) sample of $[Pt(AuPPh_3)_8](NO_3)_2$ was dissolved in 5 mL of dichloromethane. Dihydrogen was bubbled through this brown solution for 10 min, after which 2.0 mg (0.020 mmol) of CuCl was added. The solution, which had turned red, was stirred for 1 h under dihydrogen atmosphere. The clear solution was then evaporated to dryness under reduced pressure to yield a brown-red solid. The ^{31}P NMR spectrum of this solid mainly revealed the presence of **2** and $[Pt(AuPPh_3)_8]^{2+}$ and some minor amounts of **1**. Mind the difference with a similar procedure to prepare **1** (see above), where acetone was used as the solvent instead of dichloromethane (see Results and Discussion).

(D) A sample of 100 mg (0.025 mmol) $[Pt(AuPPh_3)_8](NO_3)_2$ was dissolved in 4 mL of methanol, and dihydrogen was bubbled through this solution for 10 min, upon which the color changed from brown to red-brown. A 2.7-mg (0.027-mmol) sample of CuCl was added under dihydrogen atmosphere. The color changed to dark brown, and after 1 h of stirring an orange-red precipitate formed. The reaction was then stirred for 5 h more, after which the dihydrogen atmosphere was replaced by air. The orange-red precipitate was filtered off, and it was washed with methanol and diethyl ether. Red crystals of $[Pt(H)(CuCl)_2(AuPPh_3)_8](NO_3)$ (**2**) were obtained by slow diffusion of diethyl ether into a 1:1 (v/v) dichloromethane−methanol solution of the sample (yield: 48 mg, 0.012 mmol; 87%, calculated for Cu). It should be noted that this procedure to prepare **2** is similar to the procedure to

(11) Bour, J. J.; Kanters, R. P. F.; Schlebos, P. P. J.; Steggerda, J. J. *Recl. Trav. Chim. Pays-Bas* **1988**, *107*, 211.
(12) Boyle, P. D.; Johnson, B. J.; Alexander, B. D.; Casalnuovo, J. A.; Gannon, P. R.; Johnson, S. M.; Larka, E. A.; Mueting, A. M.; Pignolet, L. H. *Inorg. Chem.* **1987**, *26*, 1346.
(13) Malatesta, L.; Naldini, L.; Simonetta, G.; Cariati, F. *Coord. Chem. Rev.* **1966**, *1*, 255.
(14) Kowala, C.; Swan, J. M. *Aust. J. Chem.* **1966**, *19*, 547.
(15) Keller, R. N.; Wycoff, H. D. *Inorg. Synth.* **1946**, *2*, 1.
(16) Costa, G.; Reisenhofer, E.; Stefani, L. *J. Inorg. Nucl. Chem.* **1965**, *27*, 2581.
(17) Kanters, R. P. F.; Bour, J. J.; Schlebos, P. P. J.; Bosman, W. P.; Behm, H.; Steggerda, J. J.; Ito, L. N.; Pignolet, L. H. *Inorg. Chem.* **1989**, *28*, 2591.

prepare **1** (see above); the major difference is the use of methanol as the solvent instead of acetone (see Results and Discussion).

Anal. Calcd for $PtAu_8Cu_2P_8C_{144}H_{121}NO_3Cl_2$ (mol wt 4130.15): C, 41.88; H, 2.95; N, 0.34. Found: C, 41.55; H, 2.91; N, 0.39. ICP: Pt:Au:Cu = 1:7.9:2.0. IR: in addition to the bands characteristic for the PPh_3 ligands, only absorption bands due to uncoordinated NO_3 (1353 cm^{-1}, broad) and the Cu−Cl stretching vibration (327 cm^{-1}) were observed. ^{31}P NMR: δ = 56.3 ppm with $^2J(P-^{195}Pt)$ (doublet) = 390 Hz. ^{195}Pt NMR: δ = −6399 ppm with $^1J(Pt-^1H)$ (doublet) = 597 Hz and $^2J(Pt-^{31}P)$ (nonet) = 390 Hz.

[Pt(H)(AuPy)(AuPPh$_3$)$_8$](NO$_3$)$_2$ (3). A sample of 100 mg (0.025 mmol) of $[Pt(AuPPh_3)_8](NO_3)_2$ was dissolved in 5 mL of pyridine. Dihydrogen was bubbled through this solution for 10 min, which changed the color from brown to dark red. To this solution was added 26 mg (0.050 mmol) of $AuPPh_3NO_3$ under dihydrogen atmosphere. This reaction mixture was stirred for 2 h, and the color changed to deep red, after which the dihydrogen atmosphere was replaced by air. Diethyl ether (80 mL) was added to give an orange-yellow precipitate which was filtered off. This residue was washed four times with 20 mL of hexane and three times with 15 mL of diethyl ether. Finally the orange-yellow powder was placed in dynamic vacuum (less than 10^{-3} mbar) for 6 h. Red crystals of $[Pt(H)(AuPy)(AuPPh_3)_8](NO_3)_2$ (**3**) were obtained by slow diffusion of a methanol solution of the product in diethyl ether (yield: 98 mg, 0.023 mmol; 92%, calculated for Pt).

The same product, **3**, was also obtained using equimolar amounts of $[Pt(AuPPh_3)_8](NO_3)_2$ and $AuPPh_3NO_3$ in the above-mentioned procedure (i.e., 100 mg (0.025 mmol) $[Pt(AuPPh_3)_8](NO_3)_2$ and 13 mg (0.025 mmol) $AuPPh_3NO_3$); the yield of this reaction (85%) is only slightly less than for the above-mentioned procedure.

Anal. Calcd for $PtAu_9P_8C_{149}H_{126}N_3O_6$ (mol wt 4270.22): C, 41.91; H, 2.97; N, 0.98. Found: C, 41.11; H, 3.00; N, 1.08. ICP: Pt:Au:P = 1:8.9:8.1. IR: in addition to the numerous bands characteristic for the PPh_3 ligands only an absorption band due to uncoordinated NO_3 (1359 cm^{-1}) could be assigned. ^{31}P NMR: δ = 52.3 ppm with $^2J(P-^{195}Pt)$ (doublet) = 388 Hz. ^1H NMR (hydride): δ = +1.4 ppm with $^3J(H-^{31}P)$ (nonet) = 13 Hz and $^1J(H-^{195}Pt)$ (doublet) = 665 Hz. ^{195}Pt NMR: δ = −6410 ppm with $^1J(Pt-^1H)$ (doublet) = 665 Hz and $^2J(Pt-^{31}P)$ (nonet) = 388 Hz.

[Pt(H)(AuPy)(AuPPh$_3$)$_8$](PF$_6$)$_2$ (3a). A 50-mg (0.012-mmol) sample of **3** was dissolved in 2 mL of methanol; to this red solution was added 50 mg (0.13 mmol) of tetra-*n*-butylammoniumhexafluorophosphate (TBAH) dissolved in 1 mL of methanol. This solution was then concentrated by evaporation until an orange-yellow precipitate of $[Pt(H)(AuPy)(AuPPh_3)_8](PF_6)_2$ formed. This precipitate was filtered off and washed with some drops of methanol. Finally it was dried in vacuum for 3 h (yield: 36 mg, 0.0082 mmol; 70%, calculated for Pt).

Anal. Calcd for $PtAu_9P_{10}C_{149}H_{126}NF_{12}$ (mol wt 4436.14): C, 40.34; H, 2.86; N, 0.32. Found: C, 39.82; H, 2.78; N, 0.38. IR: in addition to the bands originating from the PPh_3 ligands, an absorption band characteristic for PF_6 (840 cm^{-1}) was observed; bands from (uncoordinated) NO_3 were not present. ^{31}P NMR: δ = 52.3 ppm with $^2J(P-^{195}Pt)$ (doublet) = 388 Hz.

[Pt(H)(AuCl)(AuPPh$_3$)$_8$](NO$_3$) (4a). (A) A 60-mg (0.015-mmol) sample of $[Pt(AuPPh_3)_8](NO_3)_2$ was dissolved in 5 mL of pyridine under dihydrogen atmosphere. To this dark red solution was added 15 mg (0.030 mmol) of $AuPPh_3Cl$, and the mixture was stirred for 2 h. After this period the dihydrogen atmosphere was replaced by air, and 50 mL of diethyl ether was added to precipitate the orange-yellow $[Pt(H)(AuCl)(AuPPh_3)_8](NO_3)$ (**4a**) which was filtered off and washed with hexane and diethyl ether (yield: 47 mg, 0.011 mmol; 75%, calculated for Pt).

(B) A 50-mg (0.012-mmol) sample of **3** was dissolved in 1 mL of methanol. To this red solution a saturated solution of NaCl (or Et_4NCl) in methanol was added until the formation of an orange-yellow precipitate was complete. This precipitate of **4a** was filtered off and washed with some drops of methanol (yield: 46 mg, 0.011 mmol; 94%, calculated for Pt).

ICP analysis: Pt:Au:P = 1:8.8:8.0. IR: the absorption band of uncoordinated NO_3 (1360 cm^{-1}, broad) was observed in addition to the bands originating from the PPh_3 ligands. ^{31}P NMR: δ = 51.5 ppm with $^2J(P-^{195}Pt)$ (doublet) = 393 Hz.

[Pt(H)(AuBr)(AuPPh$_3$)$_8$](Br) (4b). A saturated solution of KBr in methanol was added to a solution of 50 mg (0.012 mmol) of **3** in 1 mL of methanol. The addition of this methanolic KBr solution was stopped when the formation of the orange-yellow precipitate of **4b** was complete. This orange-yellow precipitate was filtered off and washed with some drops of methanol (yield: 44 mg, 0.010 mmol; 89%, calculated for Pt).

ICP analysis: Pt:Au:P = 1:9.1:7.8. IR: characteristic absorption bands originating from the PPh_3 ligands; the absorption band of NO_3 is absent, which points toward Br^- as counteranion for **4b** (the insolubility of **4b** in apolar solvents like toluene and benzene is taken as an indication that this cluster compound is ionic, see Results and Discussion). ^{31}P NMR: δ = 51.4 ppm with $^2J(P-^{195}Pt)$ (doublet) = 393 Hz.

This cationic cluster compound was also obtained from the reaction of $[Pt(AuPPh_3)_8]^{2+}$ with Br^- in refluxing ethanol.[18] However, the reproducibility and the yield of this reaction were rather poor.

The reaction between $[Pt(AuPPh_3)_8](NO_3)_2$ and $AuPPh_3Br$ in pyridine under dihydrogen atmosphere, analogous to method A for cluster compound **4a** (see above), did not result in the desired product **4b** but yielded several unidentified products.

[Pt(H)(AuSCN)(AuPPh$_3$)$_8$](SCN) (4c). To a solution of 50 mg (0.012 mmol) of **3** in 1 mL of methanol was added a solution of 4.0 mg (0.041 mmol) of KSCN in 1 mL of methanol. This yielded an orange-yellow precipitate of **4c** that was filtered off and washed with methanol (yield: 35 mg, 0.0084 mmol; 70%, calculated for Pt).

ICP analysis: Pt:Au:P = 1:9.0:8.1. IR: in addition to the bands originating from the PPh_3 ligands, the ν(CN) from coordinated thiocyanate (2099 cm^{-1}) as well as that from ionic thiocyanate (2050 cm^{-1}) was observed. ^{31}P NMR: δ = 51.5 ppm with $^2J(P-^{195}Pt)$ (doublet) = 390 Hz.

[Pt(H)(PPh$_3$)(CuCl)(AuPPh$_3$)$_6$]$^+$ (5). This synthesis was carried out using standard Schlenk techniques, under an atmosphere of dry nitrogen.

A 200-mg (0.053-mmol) sample of $[Pt(H)(PPh_3)(AuPPh_3)_7](NO_3)_2$ and a 38-mg (0.026-mmol) sample of $[PPh_3CuCl]_4$ were dried in vacuum (less than 10^{-3} mbar) for 1 h; 5 mL of dichloromethane was then added, and this red mixture was stirred vigorously. After 1 day the red solution was concentrated to a volume of 2 mL by evaporation; this was then purified by column chromatography on alumina (Merck, Aluminiumoxide 90 Active, neutral, activity III) with a 0.01 M tetra-*n*-butylammoniumhexafluorophosphate (TBAH) solution in dichloromethane as eluting agent. The red frontlayer in this column was collected, and this solution was evaporated to dryness under reduced pressure. Analysis showed that this red product consists of cluster compound **5**, together with TBAH, originating from the eluting agent (yield of **5** is 60−70%, as estimated from ^{31}P NMR spectra of crude products).

Due to the presence of TBAH in the final product, compound **5** has not been analyzed by elemental C, H, and N analysis. ICP: Pt:Au:Cu = 1:6.2:1.1. IR: absorption bands of uncoordinated NO_3 (1378 cm^{-1}, broad) as well as of PF_6 (840 cm^{-1}) were observed in addition to several bands originating from the PPh_3 ligands and the tetra-*n*-butylammonium ion. ^{31}P NMR: Au*P* δ = 49.8 ppm with $^2J(P-^{195}Pt)$ (doublet) = 410 Hz and $^3J(P-P)$ (doublet) = 28 Hz; Pt*P* δ = 56.1 ppm with $^1J(P-^{195}Pt)$ (doublet) = 2642 Hz and $^3J(P-P)$ (septet) = 28 Hz. ^1H NMR (hydride): δ = +0.46 ppm with $^1J(H-^{195}Pt)$ (doublet) = 606 Hz, $^2J(H-^{31}P)$ (doublet) = 8 Hz and $^3J(H-^{31}P)$ (septet) = 22 Hz. ^{195}Pt NMR: δ = −5566 ppm with $^1J(Pt-^1H)$ (doublet) = 606 Hz, $^1J(Pt-^{31}P)$ (doublet) = 2642 Hz and $^2J(Pt-^{31}P)$ (septet) = 410 Hz. The FAB-MS spectrum of **5** is in agreement with its composition (see Results and Discussion).

Cluster **5** was also obtained when using $[PPh_3CuBr]_4$ or $[PPh_3CuI]_4$ instead of $[PPh_3CuCl]_4$ in the above-mentioned preparation. This is most likely due to halide exchange with Cl^- from dichloromethane on the alumina column, since donation of Cl^- by dichloromethane is also known from other reactions.[10]

Structure Determination of [Pt(H)(CuCl)(AuPPh$_3$)$_8$](NO$_3$) (1) and [Pt(H)(CuCl)$_2$(AuPPh$_3$)$_8$](NO$_3$) (2). Collection and Reduction of

(18) Schoondergang, M. F. J. New Developments in Platinum-Gold Cluster Chemistry. Thesis, University of Nijmegen, Nijmegen, 1992.

Table 1. Crystal Data for $[Pt(H)(CuCl)(AuPPh_3)_8](NO_3)$ (**1**) and $[Pt(H)(CuCl)_2(AuPPh_3)_8](NO_3)$ (**2**)

	1	**2**
chem formula[a]	$PtAu_8CuP_8C_{144}H_{121}ClNO_3$	$PtAu_8Cu_2P_8C_{144}H_{121}Cl_2NO_3$
fw	4031.1	4130.1
a/Å	15.284(8)	15.349(4)
b/Å	26.004(2)	16.949(2)
c/Å	16.558(2)	29.037(7)
α/deg		78.95(1)
β/deg	95.27(5)	74.87(2)
γ/deg		84.74(2)
V/Å^3	6636	7150
Z	2	2
space group	$P2_1$ (No.4)	$P\bar{1}$ (No.2)
T/°C	20	20
λ/Å	0.7107	0.7107
ϱ_{calc}/g·cm^{-3}	not calculated because of uncertainty in solvent content	
μ(Mo Kα)/cm^{-1} [a]	102.9	96.0
R^b [$I > 2\sigma(I)$]	0.083	0.085
wR_2^c [$I > 2\sigma(I)$]	0.18	0.22

[a] Solvent molecules not included. [b] $R = \sum||F_o| - |F_c||/\sum|F_o|$. [c] $wR_2 = [\sum w(F_o^2 - F_c^2)^2/\sum w(F_o^2)^2]^{1/2}$.

Crystallographic Data. Since single crystals decomposed very quickly upon removal from the solvent mixture, crystals of **1** and **2** were mounted in a capillary together with a mixture of methanol, dichloromethane and diethyl ether. X-ray data were measured on a Nonius CAD4 diffractometer. Standard experimental details are given elsewhere.[19] Emperical absorption corrections based on a Ψ scan were performed (see Supplementary Material). Crystal data for **1** and **2** are listed in Table 1.

Solution and Refinement of the Structures. $[Pt(H)(CuCl)(AuPPh_3)_8](NO_3)$ (1). The structure was partially solved in space group $P2_1/m$. The positions of the metal atoms were found from automatic Patterson interpretation (PATTY[20]) followed by a phase refinement procedure to expand the fragment (DIRDIF[21]). Most of the phenyl rings were positioned from successive difference Fourier maps, but some phenyl rings appeared to be disordered due to the presence of the crystallographic mirror plane through the molecule. At this stage the structure evaluation continued in space group $P2_1$. Nevertheless, some disorder in the phenyl rings remained and neither the NO_3^- ion nor any of the solvent molecules could be identified unambiguously. The observed disorder can easely be caused by the local mirror symmetry of the metal atoms.

The structure was refined by full-matrix least-squares on F_o^2 values using SHELXL[22] with anisotropic parameters for the metal, phosphorus, and chlorine atoms. The phenyl rings were refined with restrained idealized geometry, (flat, with twofold symmetry) three of which in disordered orientations. The hydrogen atoms of the phenyl rings were placed at calculated positions (C−H = 0.93 Å). After refinement to an *R* value of 0.13, an additional empirical absorption correction based on $F_o - |F_c|$ was applied using DIFABS[23] on the original unmerged F_o values. Convergence was reached at $R = 0.083$ (on *F* values, $F_o > 4\sigma(F_o)$) and $R_wF^2 = 0.18$ (on F^2 values, including all reflections). The first 100 rest peaks in the last difference Fourier map were in the range 2.3−0.90 e/Å^3; 37 of these peaks were within a distance of 2 Å from the metal atoms, and 17 peaks had a distance more than 2.5 Å from any atom of the cluster molecule. The latter may be atoms of the NO_3^- ion or the solvent molecules; refining these peaks as carbon atoms did not improve the overall geometry of the cluster, and therefore these peaks were discarded. Other peaks in the neighborhood of the phenyl rings are the result of unresolved disorder in the phenyl rings, which also explains the occurence of several very short interphenyl C−C distances (see Supplementary Material). The function minimized was $\sum w(F_o^2 - F_c^2)^2$ with $w = 1/[\sigma^2(F_o^2) + (0.0585F_c^2)^2]$.

Positional and thermal parameters of selected atoms are given in Table 2, and selected bond distances and bond angles are given in Table 3. The molecular structure of **1** is given in Figure 1.[24]

$[Pt(H)(CuCl)_2(AuPPh_3)_8](NO_3)$ (2). The positions of the non-hydrogen atoms were found from an automatic orientation and translation search (ORIENT,[25] TRACOR[26]) with a $PtAu_8Cu$ fragment of **1** as a search model, followed by a phase refinement procedure to

Table 2. Selected Atomic Coordinates (×10^4) and Equivalent Isotropic Displacement Parameters (Å^2 × 10^3) for **1**[a]

	x	*y*	*z*	U_{eq}
Au(1)	2624(1)	116(2)	4279(1)	68(1)
Au(2)	2970(2)	−475(1)	1575(2)	56(1)
Au(3)	2919(2)	705(1)	1584(1)	66(1)
Au(4)	3100(2)	946(1)	3339(2)	56(1)
Au(5)	1331(3)	−734(1)	2540(2)	82(1)
Au(6)	1184(1)	109(1)	1363(1)	39(1)
Au(7)	3089(2)	−742(1)	3300(2)	44(1)
Au(8)	1317(2)	924(1)	2558(2)	91(1)
Pt(1)	2299(1)	99(1)	2684(1)	29(1)
Cu(1)	3973(2)	87(4)	2818(2)	45(1)
Cl(1)	5371(7)	286(3)	2909(6)	60(3)
P(1)	2489(5)	117(7)	5638(4)	52(2)
P(2)	3341(7)	−1051(4)	584(6)	51(3)
P(3)	3866(7)	1185(4)	828(6)	48(3)
P(4)	3913(9)	1623(5)	3894(8)	58(5)
P(5)	114(7)	−1223(4)	2968(7)	61(3)
P(6)	132(5)	85(6)	285(4)	47(2)
P(7)	3793(9)	−1385(4)	4076(8)	56(4)
P(8)	335(8)	1563(4)	2416(7)	64(3)

[a] U_{eq} is defined as one-third of the trace of the orthogonalized U_{ij} tensor.

Table 3. Selected Bond Lengths (Å) and Bond Angles (deg) for $[Pt(H)(CuCl)(AuPPh_3)_8](NO_3)$ (**1**)

Au(1)−Au(4)	2.795(5)	Au(6)−Pt(1)	2.647(2)
Au(1)−Au(7)	2.884(5)	Au(7)−Pt(1)	2.656(4)
Au(2)−Au(3)	3.070(2)	Au(8)−Pt(1)	2.616(4)
Au(2)−Au(5)	3.165(5)	Au(2)−Cu(1)	2.855(8)
Au(2)−Au(6)	3.116(4)	Au(3)−Cu(1)	2.958(7)
Au(2)−Au(7)	2.930(4)	Au(4)−Cu(1)	2.778(10)
Au(3)−Au(4)	2.960(4)	Au(7)−Cu(1)	2.704(9)
Au(3)−Au(6)	3.066(4)	Au(1)−P(1)	2.279(7)
Au(3)−Au(8)	3.105(5)	Au(2)−P(2)	2.328(9)
Au(4)−Au(8)	2.908(5)	Au(3)−P(3)	2.356(10)
Au(5)−Au(6)	2.926(4)	Au(4)−P(4)	2.297(12)
Au(5)−Au(7)	2.860(5)	Au(5)−P(5)	2.414(10)
Au(6)−Au(8)	2.894(4)	Au(6)−P(6)	2.291(7)
Au(1)−Pt(1)	2.642(2)	Au(7)−P(7)	2.313(10)
Au(2)−Pt(1)	2.646(3)	Au(8)−P(8)	2.236(10)
Au(3)−Pt(1)	2.647(3)	Pt(1)−Cu(1)	2.548(4)
Au(4)−Pt(1)	2.698(4)	Cu(1)−Cl(1)	2.189(11)
Au(5)−Pt(1)	2.621(4)	Cu(1)−Au(1)	3.320(4)
Au(1)−Pt(1)−Au(4)	63.10(12)	Au(1)−Pt(1)−Cu(1)	79.50(10)
Au(1)−Pt(1)−Au(5)	99.07(14)	Au(2)−Pt(1)−Cu(1)	66.7(2)
Au(1)−Pt(1)−Au(7)	65.97(12)	Au(3)−Pt(1)−Cu(1)	69.4(2)
Au(1)−Pt(1)−Au(8)	96.87(14)	Au(4)−Pt(1)−Cu(1)	63.9(2)
Au(2)−Pt(1)−Au(3)	70.90(5)	Au(7)−Pt(1)−Cu(1)	62.6(2)
Au(2)−Pt(1)−Au(5)	73.86(13)	Pt(1)−Au(1)−P(1)	164.0(2)
Au(2)−Pt(1)−Au(6)	72.14(9)	Pt(1)−Au(2)−P(2)	170.6(3)
Au(2)−Pt(1)−Au(7)	67.09(11)	Pt(1)−Au(3)−P(3)	163.0(3)
Au(3)−Pt(1)−Au(4)	67.24(11)	Pt(1)−Au(4)−P(4)	174.2(4)
Au(3)−Pt(1)−Au(6)	70.77(9)	Pt(1)−Au(5)−P(5)	148.5(3)
Au(3)−Pt(1)−Au(8)	72.3(2)	Pt(1)−Au(6)−P(6)	175.1(2)
Au(4)−Pt(1)−Au(8)	66.35(13)	Pt(1)−Au(7)−P(7)	168.6(4)
Au(5)−Pt(1)−Au(6)	67.47(10)	Pt(1)−Au(8)−P(8)	172.8(4)
Au(5)−Pt(1)−Au(7)	65.63(13)	Pt(1)−Cu(1)−Cl(1)	165.6(6)
Au(6)−Pt(1)−Au(8)	66.73(11)		

(19) Smits, J. M. M.; Behm, H.; Bosman, W. P.; Beurskens, P. T. *J. Crystallogr. Spectrosc. Res.* **1988**, *18*, 447.
(20) Admiraal, G.; Behm, H.; Smykalla, C.; Beurskens, P. T. *Z. Kristallogr., Suppl.* **1992**, *6*, 522.
(21) Beurskens, P. T.; Admiraal, G.; Beurskens, G.; Bosman, W. P.; Garcia-Granda, S.; Gould, R. O.; Smits, J. M. M.; Smykalla, C. *The DIRDIF Program System, Technical Report of the Crystallography Laboratory*, University of Nijmegen: Nijmegen, The Netherlands, 1992.
(22) Sheldrick, G. M. *SHELXL-92, Program for the Refinement of Crystal Structures*, University of Goettingen: Goettingen, Germany, 1992.
(23) Walker, N.; Stuart, D. *Acta Crystallogr.* **1983**, *A39*, 158.
(24) Johnson, C. K. *ORTEP-II, Report on ORNL-5138*, Oak Ridge National Laboratory: Oak Ridge, TN, 1976.

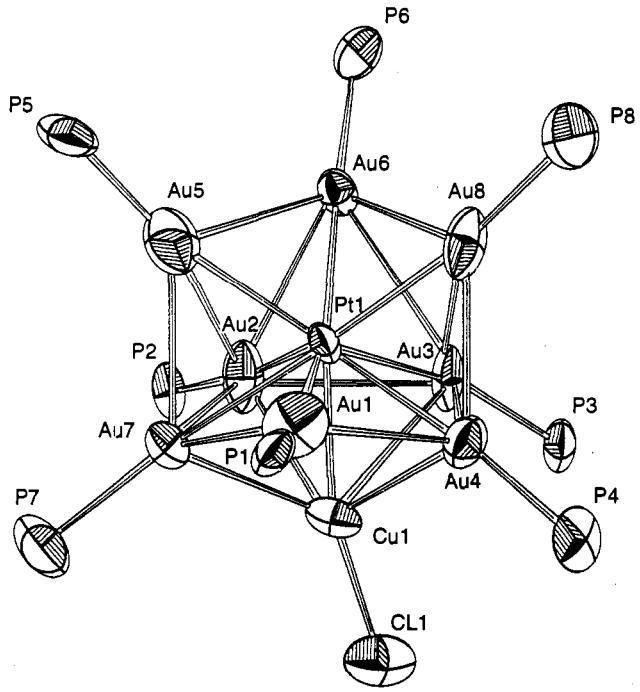

Figure 1. X-ray structure of $[Pt(H)(CuCl)(AuPPh_3)_8](NO_3)$ (**1**) with atom labeling for Pt, Au, Cu, P, and Cl. Phenyl rings and the NO_3^- ion have been omitted for the sake of clarity. Thermal ellipsoids are at 50% probability.

expand the fragment (DIRDIF[21]). The NO_3^- ion was positioned from difference Fourier maps. Of the unknown amount of solvent molecules none could be detected.

The structure was refined by full-matrix least-squares on F_o^2 values using SHELXL[22] with anisotropic parameters for the metal, phosphorus and chlorine atoms. The NO_3^- ion was refined with restrained idealized geometry (flat, 2-fold symmetry) with the hydrogen atoms of the phenyl rings placed at calculated positions (C−H = 0.93 Å).

After refinement to an R value of 0.13, an additional empirical absorption correction based on $F_o - |F_c|$ was applied using DIFABS[23] on the original unmerged F_o values. Final convergence was reached at $R = 0.085$ (on F values, $F_o > 4\sigma(F_{o0})$) and $R_wF^2 = 0.18$ (on F^2 values, including all reflections). The function minimized was $\sum w(F_o^2 - F_c^2)^2$ with $w = 1/[\sigma^2(F_o^2) + (0.078F_c^2)^2]$. A maximum residual density of 2.2 e/Å^3 was found near metal atoms.

The total volume of the solvent area was calculated to be 1057 Å^3 (14.8 vol%) (PLATON[27]). This volume is filled with unidentified solvent molecules.

Positional and thermal parameters of selected atoms are given in Table 4, and selected bond distances and bond angles are given in Table 5. The molecular structure of **2** is given in Figure 2.[24]

Results and Discussion

Synthesis, Characterization and Crystal Structure of $[Pt(H)(CuCl)(AuPPh_3)_8](NO_3)$ (1). The compound $[Pt(H)(CuCl)(AuPPh_3)_8](NO_3)$ (**1**) is obtained from the reaction of $[Pt(AuPPh_3)_8](NO_3)_2$ with dihydrogen and CuCl in acetone solution (yield: 80%). It is thought that the formation of **1** proceeds in a way analogous to that supposed for $[Pt(H)(AgNO_3)(AuPPh_3)_8](NO_3)$;[10] i.e., after oxidative addition of H_2 to $[Pt(AuPPh_3)_8]^{2+}$, one of the H-ligands of the resulting dihydride $[Pt(H)_2(AuPPh_3)_8]^{2+}$ [9] is replaced by electrophilic substitution of CuCl. **1** was characterized by means of elemental C, H, and N analysis, ICP analysis, and IR, ^{31}P NMR and ^{195}Pt NMR spectroscopy. Its solid-state structure was revealed by a single-crystal X-ray analysis.

NMR Spectroscopy. As a result of the fluxional behavior of the different phosphine sites at room temperature a singlet is observed in the ^{31}P NMR spectrum of **1**. The magnitude of $J(P-^{195}Pt)$ shows it to be a ^2J coupling, thereby indicating that

Table 4. Selected Atomic Coordinates ($\times 10^4$) and Equivalent Isotropic Displacement Parameters (Å^2 × 10^3) for **2**[a]

	x	y	z	U_{eq}
Pt(1)	1957(1)	2106(1)	2522(1)	29(1)
Au(1)	2425(1)	3577(1)	2568(1)	38(1)
Au(2)	2554(1)	804(1)	3066(1)	34(1)
Au(3)	3185(1)	1160(1)	2015(1)	34(1)
Au(4)	3075(1)	2883(1)	1713(1)	36(1)
Au(5)	483(1)	2985(1)	2897(1)	45(1)
Au(6)	1198(1)	751(1)	2526(1)	38(1)
Au(7)	2067(1)	2339(1)	3400(1)	36(1)
Au(8)	1548(1)	2027(1)	1684(1)	42(1)
Cu(1)	3552(3)	2221(3)	2586(2)	33(1)
Cu(2)	824(3)	1447(3)	3308(2)	37(1)
Cl(1)	4889(8)	2382(8)	2654(5)	58(3)
Cl(2)	−88(9)	969(9)	3983(4)	62(3)
P(1)	2711(8)	4907(6)	2498(4)	42(2)
P(2)	3125(7)	−286(6)	3511(4)	38(2)
P(3)	4311(8)	339(6)	1609(4)	45(2)
P(4)	3864(7)	3630(6)	1011(4)	35(2)
P(5)	−865(8)	3695(8)	3053(6)	59(3)
P(6)	212(8)	−224(7)	2653(5)	43(2)
P(7)	2126(8)	2563(7)	4141(4)	40(2)
P(8)	1014(9)	2149(8)	1001(4)	49(3)

[a] U_{eq} is defined as one third of the trace of the orthogonalized U_{ij} tensor.

Table 5. Selected Bond Lengths (Å) and Bond Angles (deg) for $[Pt(H)(CuCl)_2(AuPPh_3)_8](NO_3)$ (**2**)

Pt(1)−Au(1)	2.650(2)	Au(5)−Au(7)	3.161(2)
Pt(1)−Au(2)	2.693(2)	Au(6)−Au(8)	2.906(2)
Pt(1)−Au(3)	2.681(2)	Au(2)−Cu(2)	2.742(5)
Pt(1)−Au(4)	2.705(2)	Au(2)−Cu(1)	2.887(5)
Pt(1)−Au(5)	2.691(2)	Au(3)−Cu(1)	2.849(5)
Pt(1)−Au(6)	2.665(2)	Au(4)−Cu(1)	2.821(5)
Pt(1)−Au(7)	2.705(2)	Au(5)−Cu(2)	2.716(5)
Pt(1)−Au(8)	2.695(2)	Au(6)−Cu(2)	2.663(5)
Pt(1)−Cu(1)	2.532(5)	Au(7)−Cu(1)	2.848(5)
Pt(1)−Cu(2)	2.605(5)	Au(7)−Cu(2)	2.636(5)
Au(1)−Cu(1)	2.749(5)	Au(1)−P(1)	2.296(10)
Au(1)−Au(4)	2.856(2)	Au(2)−P(2)	2.288(10)
Au(1)−Au(5)	3.081(3)	Au(3)−P(3)	2.332(10)
Au(1)−Au(7)	2.851(2)	Au(4)−P(4)	2.286(10)
Au(2)−Au(3)	2.910(2)	Au(5)−P(5)	2.280(11)
Au(2)−Au(6)	2.931(2)	Au(6)−P(6)	2.256(11)
Au(2)−Au(7)	2.916(2)	Au(7)−P(7)	2.279(11)
Au(3)−Au(4)	2.886(2)	Au(8)−P(8)	2.305(12)
Au(3)−Au(6)	3.101(2)	Cu(1)−Cl(1)	2.159(12)
Au(3)−Au(8)	3.072(2)	Cu(2)−Cl(2)	2.152(12)
Au(4)−Au(8)	2.893(2)		

Au(1)−Pt(1)−Au(4)	63.85(6)	Au(2)−Pt(1)−Cu(2)	62.31(12)
Au(1)−Pt(1)−Au(5)	69.79(6)	Au(3)−Pt(1)−Cu(1)	66.19(12)
Au(1)−Pt(1)−Au(7)	63.73(6)	Au(4)−Pt(1)−Cu(1)	65.08(12)
Au(2)−Pt(1)−Au(3)	65.58(5)	Au(5)−Pt(1)−Cu(2)	61.67(12)
Au(2)−Pt(1)−Au(6)	66.33(6)	Au(7)−Pt(1)−Cu(1)	65.80(12)
Au(2)−Pt(1)−Au(7)	65.39(6)	Au(7)−Pt(1)−Cu(2)	59.48(12)
Au(3)−Pt(1)−Au(6)	70.92(6)	Pt(1)−Au(1)−P(1)	170.2(3)
Au(3)−Pt(1)−Au(8)	69.71(6)	Pt(1)−Au(2)−P(2)	177.5(3)
Au(3)−Pt(1)−Au(4)	64.79(5)	Pt(1)−Au(3)−P(3)	176.3(3)
Au(4)−Pt(1)−Au(8)	64.78(6)	Pt(1)−Au(4)−P(4)	172.9(3)
Au(5)−Pt(1)−Au(7)	71.72(6)	Pt(1)−Au(5)−P(5)	166.3(4)
Au(6)−Pt(1)−Au(8)	65.67(6)	Pt(1)−Au(6)−P(6)	163.9(3)
Au(1)−Pt(1)−Cu(1)	63.37(12)	Pt(1)−Au(7)−P(7)	178.3(3)
Au(6)−Pt(1)−Cu(2)	60.71(12)	Pt(1)−Cu(1)−Cl(1	176.8(5)
Au(2)−Pt(1)−Cu(1)	66.99(12)	Pt(1)−Cu(2)−Cl(2	175.8(5)

(25) Beurskens, P. T.; Beurskens, G.; Strumpel, M.; Nordman, C. E. *Patterson and Pattersons*; Glusker, J. P., Patterson, B. K., Rossi, M., Eds.; Clarendon Press: Oxford, U.K., 1987; p 356.
(26) Beurskens, P. T.; Gould, R. O.; Bruins Slot, H. J.; Bosman, W. P. Z. *Kristallogr.* **1987**, *179*, 127.
(27) Spek, A. L. *PLATON-93*; Bijvoet Center for Biomolecular Research, University of Utrecht: Utrecht, The Netherlands, 1993.

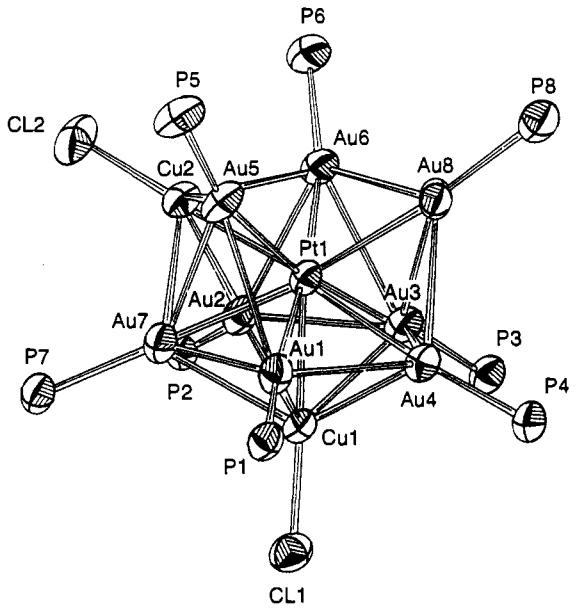

Figure 2. X-ray structure of $[Pt(H)(CuCl)_2(AuPPh_3)_8](NO_3)$ with atom labeling for Pt, Au, Cu, P, and Cl. Phenyl rings and the NO_3^- ion have been omitted for the sake of clarity. Thermal ellipsoids are at 50% probability.

the platinum atom is occupying the central position surrounded by $AuPPh_3$ units (vide infra).

^{31}P and ^{195}Pt NMR data are given in Table 6. The ^{195}Pt NMR spectrum of **1**, with $\delta = -6015$ ppm, is typically located for an $(S^\sigma)^2(P^\sigma)^6$ cluster compound upfield of −5400 ppm. Cluster compounds with an $(S^\sigma)^2(P^\sigma)^4$ electron configuration on the other hand are typically observed downfield of −4500 ppm. Phosphorus decoupling of the ^{195}Pt NMR spectrum of **1** results in a doublet due to $^1J(Pt-^1H) = 678$ Hz. The magnitude of this coupling is in the range normally observed for hydride containing PtM compounds in which the hydride is bridging between the platinum and the metal atom M.[28-34] This is in agreement with the absence of a terminal Pt−H stretching vibration (in the 2300−1700 cm^{-1} range) in the IR spectrum of **1**. The region where bridging hydrides may be observed in IR spectra (1400−800 cm^{-1}) is obscured for **1** due to the absorption bands of the PPh_3 ligands and the NO_3^-.

The presence of eight $AuPPh_3$ units bonded to the central platinum atom of **1** is concluded from the nonet structure with $^2J(Pt-^{31}P) = 410$ Hz in the $^{195}Pt\{^1H\}$ NMR spectrum.

Crystal Structure. The solid-state structure of **1** as revealed by X-ray analysis (Figure 1) shows that the cluster framework is analogous to that reported for $[Pt(H)(AgNO_3)(AuPPh_3)_8](NO_3)$.[10] The platinum atom, which is in the central position as seen from the NMR data, is surrounded by eight $AuPPh_3$ units and one CuCl unit. The metal core of **1** is clearly derived from an icosahedral (spheroidal) geometry, the copper atom is positioned at the bottom-vertex of the icosahedron, and the eight gold atoms are situated at eight adjacent vertices. Three adjacent vertices of the fictitious icosahedron therefore are not occupied by any metal atom, and they define the region that is most likely occupied by the hydride ligand, bridging between platinum and gold atoms. The copper atom, which is less electronegative than gold, is situated "trans" to the region where the relatively electronegative H ligand resides.

The Pt−Au distances (2.616 Å to 2.698 Å) and the Au−Cu distances (2.704 Å to 2.958 Å) are in the normal range for Cu−Au bonding, only the Au(1)−Cu(1) distance, 3.320(4) Å, is substantially longer. The Pt−Cu distance (2.548(4) Å) is short as compared to other known Pt−Cu distances.[5,36-38]

In the crystalline state no nitrates were located within coordinating distances from any metal atom; this is also concluded from the IR spectrum where no coordinated NO_3 is observed. The presence of a Cu−Cl stretching vibration could not be detected in the IR spectrum of **1**; this is also the case for other PtAuCu clusters containing only one CuCl unit.[5] However, a Cu−Cl stretching vibration for **2**, in which two CuCl units are present, can be assigned (vide infra).

Synthesis, Characterization, and Crystal Structure of $[Pt(H)(CuCl)_2(AuPPh_3)_8](NO_3)$ (2). The reaction of $[Pt(AuPPh_3)_8](NO_3)_2$ with CuCl, in a molar ratio of 1:2, under dihydrogen atmosphere in acetone, methanol, or dichloromethane yields the cluster compound $[Pt(H)(CuCl)_2(AuPPh_3)_8](NO_3)$ (**2**). **2** was also obtained from the reaction of $[Pt(AuPPh_3)_8](NO_3)_2$ with CuCl in a molar ratio of 1:1 under dihydrogen atmosphere in methanol or dichloromethane. However, this reaction in acetone yields cluster **1** as seen in the previous section.

The reaction between $[Pt(CuCl)(AuPPh_3)_8](NO_3)_2$ and dihydrogen in methanol or dichloromethane results in the formation of **2** and $[Pt(AuPPh_3)_8](NO_3)_2$ in equimolar amounts. Monitoring this reaction with ^{31}P NMR spectroscopy shows that **1** is present during the early stages of this reaction and that $[Pt(H)_2(AuPPh_3)_8]^{2+}$ is also present in the reaction mixture under dihydrogen. An intermolecular CuCl transfer reaction of **1** to yield **2** is remarkable because, as seen in the previous section, cluster **1** is a stable compound that can be recrystallized from a methanol/dichloromethane environment over several days, without any detectable formation of **2**. We therefore conclude that this intermolecular CuCl transfer reaction in methanol or dichloromethane is promoted by the presence of H^+ in the reaction mixture.[10] Electrophilic addition of H^+ to **1** is then postulated to result in minor (i.e., undetectable) amounts of a dihydride cluster that eliminates a CuCl unit which then reacts rapidly with **1**.

The Lewis acid CuCl obviously prefers addition to **1** because this is the most basic cluster present in solution. The solvent dependence may be related to the amount of dihydride $[Pt(H)_2(CuCl)(AuPPh_3)_8]^{2+}$ formed: apparently this dihydride is more pronounced in methanol and dichloromethane than it is in acetone because this has a proton affinity significantly higher than methanol and dichloromethane.[39] The absence of such a net intermolecular transfer of $AgNO_3$ for $[Pt(H)(AgNO_3)(AuPPh_3)_8](NO_3)$ might be due to the high charge of the hypothetical dihydride $[Pt(H)_2(Ag)(AuPPh_3)_8]^{3+}$.

NMR Spectroscopy. ^{31}P and ^{195} Pt NMR data are given in Table 6. The ^{31}P NMR spectrum of **2** consists of a singlet at δ

(28) Bour, J. J.; Schlebos, P. P. J.; Kanters, R. P. F.; Schoondergang, M. F. J.; Addens, H.; Overweg, A.; Steggerda, J. J. *Inorg. Chim. Acta* **1991**, *181*, 195.
(29) Bour, J. J.; Kanters, R. P. F.; Schlebos, P. P. J.; Bosman, W. P.; Behm, H.; Beurskens, P. T.; Steggerda, J. J. *Recl. Trav. Chim. Pays-Bas* **1987**, *106*, 157.
(30) Blum, T.; Braunstein, P. *Organometallics* **1989**, *8*, 2497.
(31) Jeffrey, J. C.; Parrot, M. J.; Stone, F. G. A. *J. Organomet. Chem.* **1990**, *382*, 225.
(32) Albinati, A.; Lehner, H.; Venanzi, L. M.; Wolfer, M. *Inorg. Chem.* **1987**, *26*, 3933.
(33) Ramachadran, R.; Yang, D-S.; Payne, N. C.; Puddephatt, R. J. *Inorg. Chem.* **1992**, *31*, 4236.
(34) Ramachandran, R.; Puddephatt, R. J. *Inorg. Chem.* **1993**, *32*, 2256.
(35) Chatt, J.; Shaw, B. L. *J. Chem. Soc.* **1962**, 5075.
(36) Hallam, M. F.; Mingos, D. M. P.; Adatia, T.; McPartlin, M. *J. Chem. Soc., Dalton Trans.* **1988**, 335.
(37) Braunstein, P.; Freyburger, S.; Bars, O. *J. Organomet. Chem.* **1988**, *352*, C29.
(38) Kappen, T. G. M. M.; Schlebos, P. P. J.; Bour, J. J.; Bosman, W. P.; Smits, J. M. M.; Beurskens, P. T.; Steggerda, J. J. To be submitted for publication.
(39) Aue, D. H.; Bowers, M. T. *Gas Phase Chemistry*; Bowers, M. T., Ed.; Academic Press: New York, 1979; Vol. 2, Chapter 9.

Table 6. ^{195}Pt, ^{31}P, and ^{1}H NMR Data[a,b]

	^{31}P	^{195}Pt	^{1}H
$[Pt(H)(CuCl)(AuPPh_3)_8](NO_3)$ (**1**)	$\delta = 54.1$ $^2J(^{31}P-^{195}Pt)$ (d) = 410	$\delta = -6015$ $^1J(^{195}Pt-^1H)$ (d) = 678 $^2J(^{195}Pt-^{31}P)$ (n) = 41	
$[Pt(H)(CuCl)_2(AuPPh_3)_8](NO_3)$ (**2**)	$\delta = 56.3$ $^2J(^{31}P-^{195}Pt)$ (d) = 390	$\delta = -6399$ $^1J(^{195}Pt-^1H)$ (d) = 597 $^2J(^{195}Pt-^{31}P)$ (n) = 390	
$[Pt(H)(AuPy)(AuPPh_3)_8](NO_3)_2$ (**3**)	$\delta = 52.3$ $^2J(^{31}P-^{195}Pt)$ (d) = 388	$\delta = -6410$ $^1J(^{195}Pt-^1H)$ (d) = 665 $^2J(^{195}Pt-^{31}P)$ (n) = 388	$\delta = 1.4$ $^3J(^1H-^{31}P)$ (n) = 13 $^1J(^1H-^{195}Pt)$ (d) = 665
$[Pt(H)(CuCl)(AuPPh_3)_8](PF_6)$ (**3a**)	$\delta = 52.3$ $^2J(^{31}P-^{195}Pt)$ (d) = 388		
$[Pt(H)(AuCl)(AuPPh_3)_8](NO_3)$ (**4a**)	$\delta = 51.5$ $^2J(^{31}P-^{195}Pt)$ (d) = 393		
$[Pt(H)(AuBr)(AuPPh_3)_8](Br)$ (**4b**)	$\delta = 51.4$ $^2J(^{31}P-^{195}Pt)$ (d) = 393		
$[Pt(H)(AuSCN)(AuPPh_3)_8](SCN)$ (**4c**)	$\delta = 51.5$ $^2J(^{31}P-^{195}Pt)$ (d) = 390		
$[Pt(H)(PPh3)(CuCl)(AuPPh_3)_6]^+$ (**5**)	$\delta = 49.8$ (Au−P) $^2J(^{31}P-^{195}Pt)$ (d) = 410 $^3J(^{31}P-^{31}P)$ (d) = 28 $\delta = 56.1$ (Pt−P) $^1J(^{31}P-^{195}Pt)$ (d) = 2642 $^3J(^{31}P-^{31}P)$ (s) = 28	$\delta = -5566$ $^1J(^{195}Pt-^1H)$ (d) = 606 $^1J(^{195}Pt-^{31}P)$ (d) = 2642 $^2J(^{195}Pt-^{31}P)$ (s) = 410	$\delta = 0.46$ $^1J(^1H-^{31}P)$ (d) = 606 $^2J(^1H-^{31}P)$ (d) = 8 $^3J(^1H-^{31}P)$ (s) = 22
$[Pt(H)(AuPPh_3)_8](NO_3)$ (**6**)		$\delta = -5673$ $^1J(^{195}Pt-^1H)$ (d) = 721 $^2J(^{195}Pt-^{31}P)$ (n) = 452	

[a] Chemical shifts in ppm; coupling constants in Hz. [b] Key: n = nonet, s = septet, and d = doublet.

= 56.3 ppm, due to the fluxionality of the different P-sites, with $^2J(P-^{195}Pt)$ = 390 Hz. The magnitude of this coupling is in the range normally observed for a ^2J coupling and therefore shows unambiguously that **2** has a platinum atom in central position which is surrounded by $AuPPh_3$ units.

The presence of eight $AuPPh_3$ units bonded to the central platinum atom is clear from the nonet splitting with $^2J(Pt-^{31}P)$ = 390 Hz in the $^{195}Pt\{^1H\}$ NMR spectrum. The presence of one hydride ligand in **2** is inferred from the doublet structure with $^1J(Pt-^1H)$ = 597 Hz in the $^{195}Pt\{^{31}P\}$ NMR spectrum. From the magnitude of this coupling, like for **1**, it is concluded that the hydride ligand in **2** is also bridging between the central platinum and peripheral metal atoms, most likely gold atoms as deduced from crystallographic information (vide infra).

Comparison of the three related clusters $[Pt(H)(AuPPh_3)_8](NO_3)$,[28] **1**, and **2** shows that the order for $\delta(^{195}Pt)$ is $[Pt(H)(AuPPh_3)_8](NO_3)$ > **1** > **2** (see Table 6). This sequence can be attributed to the more complete spherical surrounding of the central Pt atoms.

The scalar coupling constants between Pt and H and between Pt and P decrease in the order $[Pt(H)(AuPPh_3)_8](NO_3)$ > **1** > **2** (see Table 6). This is due to the decrease in bond order between the central Pt, the hydride, and the peripheral metal atoms in going from $[Pt(H)(AuPPh_3)_8](NO_3)$ to **1** to **2** as with the same number of bonding electrons for all three clusters, additional Pt−Cu bonds have to be maintained. This decrease in bond order in going from **1** to **2** is also reflected in the (mean) Pt−Au and Pt−Cu bond lengths of **1** and **2** (vide infra).

Crystal Structure. The X-ray structure analysis of the solid shows (Figure 2) that the metal core of **2** consists of 11 metal atoms. The central position is occupied by a platinum atom (as concluded from NMR experiments) which is surrounded by eight gold atoms and two copper atoms in an icosahedral (spheroidal) geometry. The gold atoms are all bonded to triphenylphosphine ligands, whereas both copper atoms are bonded to Cl. No close Cu−Cu contacts are observed in the solid-state geometry of **2**. The structural relationship between the cluster frameworks of **1** and **2** is clear from Figures 1 and 2. Derived from an icosahedral geometry the solid-state structure of **2** (Figure 2) has two vertices which are not occupied by any metal atom. This region clearly defines the area where the hydride ligand is to be located in a bridging position as based on spectroscopic considerations.

The Pt−Au distances (2.650−2.705 Å) as well as the Pt−Cu distances (2.532 and 2.605 Å) for **2** are, on average, significantly longer than those for **1**, which correlates with the decrease in scalar coupling constants between Pt and H and between Pt and P in going from **1** to **2**.

No nitrates were located within coordinating distances from any metal atom; this is also seen in the IR spectrum, where NO_3^- is observed at 1353 cm^{-1} (uncoordinated NO_3^-). The presence of Cu−Cl bonds is also concluded from the Cu−Cl stretching vibration (327 cm^{-1}) in the IR spectrum of **2**. The absence of a terminal Pt−H stretching vibration further supports the proposed bridging nature of the hydride ligand.

Elemental C, H, and N analysis, together with the Pt:Au:Cu ratio as obtained from ICP analysis, is in agreement with the formulation $[Pt(H)(CuCl)_2(AuPPh_3)_8](NO_3)$.

Synthesis and Characterization of $[Pt(H)(AuPy)(AuPPh_3)_8](NO_3)_2$ (3). $[Pt(H)(AuPy)(AuPPh_3)_8](NO_3)_2$ (**3**) (in which Py = C_5H_5N) is obtained in quantitative yields from the reaction of $[Pt(AuPPh_3)_8](NO_3)_2$ with $AuPPh_3NO_3$ and H_2 in pyridine. In analogy with the preparation of **1** and $[Pt(H)(AgNO_3)(AuPPh_3)_8](NO_3)$,[10] it is proposed that **3** is formed by electrophilic substitution of a hydride ligand of $[Pt(H)_2(AuPPh_3)_8](NO_3)_2$ by a d^{10}-metal unit, in this case $AuPy^+$. Due to steric arguments this electrophilic substitution is not allowed to a $AuPPh_3^+$ unit: from calculations it was concluded that the maximum number of triphenylphosphines bonded to the metal core of gold clusters comes to eight.[40,41] Coordination of pyridine to this gold atom bypasses this steric problem and apparently is preferred over coordination of nitrate. Nitrogen

(40) Steggerda, J. J.; Bour, J. J.; van der Velden, J. W. A. *Recl. Trav. Chim. Pays-Bas* **1982**, *101*, 164.
(41) Kitaigorodski, *Organic Chemical Crystallography*; Consultance Bureau: New York, 1961; p 12.

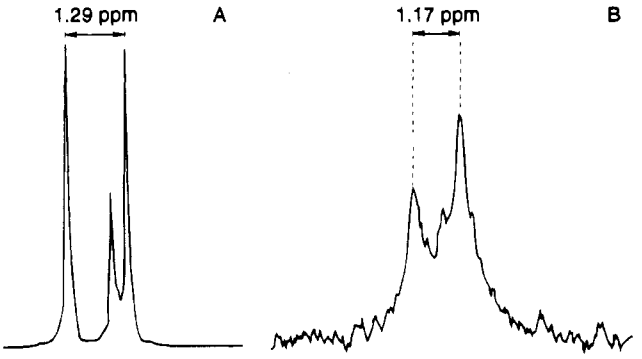

Figure 3. (A) ^{2}H-NMR spectrum of pyridine-d_5 in CH_2Cl_2 (30.722 MHz). (B) ^{2}H-NMR spectrum of **3** synthesized with pyridine-d_5 in CH_2Cl_2 (30.722 MHz) (see text).

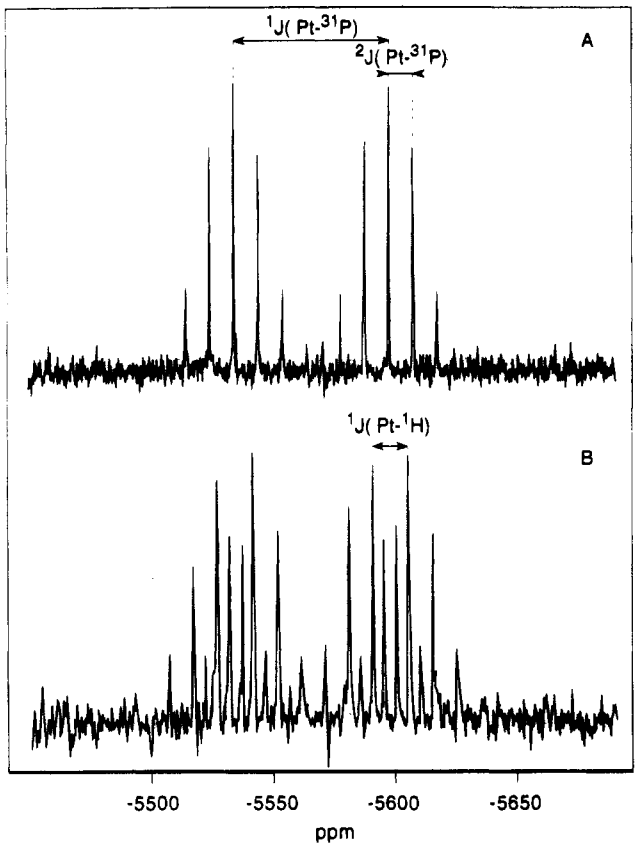

Figure 4. (A) ^{195}Pt{^{1}H} NMR spectrum and (B) ^{195}Pt NMR spectrum of $[Pt(H)(PPh_3)(CuCl)(AuPPh_3)_6]^+$ (**5**).

coordination of N-bases to gold is well-known from the literature.[42-46]

NMR Spectroscopy. ^{31}P and ^{195}Pt NMR spectroscopic data are given in Table 6. The ^{31}P NMR spectrum of **3**, which consists of a singlet at $\delta = 52.3$ ppm with a $^2J(P-^{195}Pt) = 388$ Hz, shows the presence of a central platinum atom. The magnitude of $J(P-^{195}Pt)$ is indicative of a ^2J coupling via a gold, and therefore shows that the PPh_3 groups are all coordinated to gold. The ^{195}Pt{^{1}H} NMR spectrum, a nonet located at $\delta = -6410$ ppm, shows the presence of eight $AuPPh_3$ units. The presence of a direct Pt−H bond is proved by the ^{195}Pt{^{31}P} NMR spectrum, which shows a doublet structure due to $^1J(Pt-^1H) = 665$ Hz. The magnitude of this coupling is, like for other hydride containing PtAu clusters, characteristic for a hydride bridging between platinum and gold atoms. This bridging position is in agreement with the absence of a terminal Pt−H stretching vibration in the IR spectrum. In the ^{1}H NMR spectra of **3** the hydride is observed at $\delta = +1.4$ ppm; the eight $AuPPh_3$ units cause a nonet splitting of this signal with $^3J(H-^{31}P) = 13$ Hz. The central platinum atom gives rise to two ^{195}Pt-satellite peaks with $^1J(H-^{195}Pt) = 665$ Hz. The location of this hydride resonance is a strong indication toward the bridging position of the hydride ligand, since it is known that hydride chemical shifts are observed significantly low-field on bridging.[30-33,47,48]

The pyridine resonances could not be assigned in the ^{1}H NMR spectrum due to the presence of intense PPh_3 resonances in the aromatic region.

Evidence for Pyridine Coordination to Gold. As seen from the ICP analysis of **3**, this cluster consists of nine Au atoms and eight PPh_3 groups in addition to one Pt atom. Elemental analysis of **3** is in agreement with the presence of three nitrogen atoms per molecular formula. However, when the uncoordinated nitrates of **3** were replaced by PF_6^- anions to yield **3a**, elemental analysis of this product revealed the presence of one nitrogen atom per molecular formula. The IR spectrum of **3** shows no absorption bands due to coordinated NO_3 and the IR spectrum of **3a** shows the absence of coordinated as well as of uncoordinated NO_3. These observations exclude nitrate to be the nitrogen-containing ligand coordinated to this gold atom, leaving pyridine as the probable candidate.

Pyridine-coordination has been unambiguously established by means of ^{2}H NMR experiments with **3** that has been synthesized with use of pyridine-d_5. Its ^{2}H NMR resonances are shown in Figure 3B: they are substantially broadened as compared to the resonances of free pyridine-d_5 (Figure 3A). Furthermore, the difference between the resonances for the α-position and the β-position (1.17 ppm) is significantly decreased as compared to that for free pyridine-d_5 in CH_2Cl_2 (1.29 ppm). This decrease is in the order of magnitude normally found upon coordination of pyridine-like bases;[42-44] the absolute positions of the resonances are not shifted more than approximately 0.2 ppm with respect to free pyridine-d_5. When excess Et_4NCl was added to the NMR sample in situ, to yield **4a**, the resonances of undisturbed free pyridine-d_5 were recovered. All the observations indicate coordination of the pyridine to gold. If coordination would have occurred to the central platinum atom, a violation of the $(S^\sigma)^2(P^\sigma)^6$ electron configuration of **3** would have taken place.

Synthesis and Characterization of $[Pt(H)(AuX)(AuPPh_3)_8]^+$ (4) (X = Cl, Br, or SCN). The pyridine-ligand of **3** can be substituted by Cl^-, Br^-, or SCN^- to give $[Pt(H)(AuX)(AuPPh_3)_8]^+$, in which X = Cl (**4a**), Br (**4b**) or SCN (**4c**). These products were characterized by means of ICP analysis, IR and ^{31}P NMR spectroscopy. The reactions for X = Cl and Br proceed to quantitative yields, which further support the close similarity of the products with **3**. The corresponding reaction with X = SCN has a yield of 70%.

The differences in ^{31}P NMR data for **4a**, **4b**, **4c**, and **3** are only very small (see Table 6). The cationic nature of **4a** is

(42) Bonati, F.; Burini, A.; Rosa Pietroni, B.; Bovio, B. *J. Organomet. Chem.* **1985**, *296*, 301.
(43) Berners Price, S. J.; DiMartino, M. J.; Hill, D. T.; Kuroda, R.; Mazid, M. A.; Sadler, P. J. *Inorg. Chem.* **1985**, *24*, 3425.
(44) Colacio, E.; Romerosa, A.; Ruiz, J.; Román, P.; Gutiérrez-Zorrilla, J. M.; Martínez-Ripoll, M. *J. Chem. Soc., Dalton Trans.* **1989**, 2323.
(45) Guy, J. J.; Jones, P. G.; Mays, M. J.; Sheldrick, G. M. *J. Chem. Soc., Dalton Trans.* **1977**, 8.
(46) Pill, T.; Polborn, K.; Kleinschmidt, A.; Erfle, V.; Breu, W.; Wagner, H.; Beck, W. *Chem. Ber.* **1991**, *124*, 1541.
(47) Gregson, D.; Howard, J. A. K.; Murray, M.; Spencer, J. L. *J. Chem. Soc., Chem. Commun.* **1981**, 716.
(48) Albinati, A.; Anklin, C.; Janser, P.; Lehner, H.; Matt, D.; Pregosin, P. S.; Venanzi, L. M. *Inorg. Chem.* **1989**, *28*, 1105.

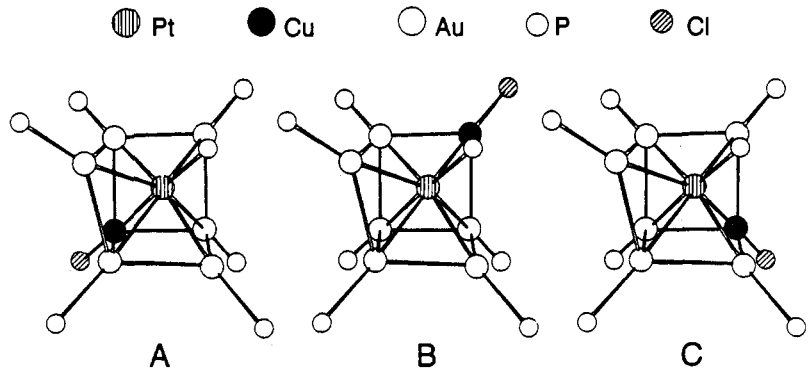

Figure 5. Three different possible isomers for **5**, assuming its $Pt(P)(M)_7$ skeleton is derived from a spheroidal, cubic geometry (see text).

Table 7. Positive Ion FAB-MS Data for **5** (M = $[Pt(H)(PPh_3)(CuCl)(AuPPh_3)_6]$)

relative mass, *m/e*[a]	% abundance	assignment
3313.2	42	$(M)^+$
3050.5	100	$(M\text{-}PPh_3)^+$
2852.8	45	$(M\text{-}Au\text{-}PPh_3\text{-}H)^+$
2788.7	82	$(M\text{-}2PPh_3)^+$
2526.3	43	$(M\text{-}3PPh_3)^+$

[a] Not matched.

seen from the presence of uncoordinated nitrate in the IR spectrum, and is in agreement with the insolubility of **4a**, **4b**, and **4c** in apolar solvents like benzene and toluene. The 1+ charge is supposed in order to obey the $(S^\sigma)^2(P^\sigma)^6$ electron configuration.

4a can also be prepared from the reaction of $[Pt(AuPPh_3)_8](NO_3)_2$ with $AuPPh_3Cl$ and H_2 in pyridine, resembling the synthesis of **3**. It is remarkable that compound **4b** could not be obtained from the reaction of $[Pt(AuPPh_3)_8](NO_3)_2$ with $AuPPh_3Br$ and H_2 in pyridine.

The absence of an absorption band of nitrate in the IR spectrum points toward Br^- as counteranion to **4b**. The IR spectrum of **4c** shows that a thiocyanate is coordinated: the C–N stretching vibration of the coordinated thiocyanate is observed at 2099 cm^{-1}, which is characteristic for a sulfur-coordinated thiocyanate.[49-52] Coordination to the central Pt atom would violate the $(S^\sigma)^2(P^\sigma)^6$ electron configuration of **4c**; therefore, it is concluded that the thiocyanate is coordinated to gold. The presence of uncoordinated, ionic thiocyanate is also clear from the IR spectrum (2050 cm^{-1} [50,51]); the absence of a nitrate vibration shows that the nitrates of **3** have been replaced by a SCN^- in **4c**.

Synthesis and Characterization of $[Pt(H)(PPh_3)(CuCl)(AuPPh_3)_6]^+$ (5). $[Pt(H)(PPh_3)(CuCl)(AuPPh_3)_6]^+$ (**5**) is obtained from the reaction between $[Pt(H)(PPh_3)(AuPPh_3)_7](NO_3)_2$ and $[PPh_3CuCl]_4$. Compound **5** is closely related to $[Pt(H)(PPh_3)(AuCl)(AuPPh_3)_6]^+$, obtained from the reaction of $[Pt(H)(PPh_3)(AuPPh_3)_7]^{2+}$ with chloride,[49] and spectroscopic data of both clusters reflect this similarity (see Table 6). It is worth noting that **5** could also be obtained by using $[PPh_3CuBr]_4$ or $[PPh_3CuI]_4$ instead of $[PPh_3CuCl]_4$. It is presumed that this is due to a halide-exchange reaction with dichloromethane on the alumina column. Donation of Cl^- by dichloromethane is also observed in other cases.[10]

Due to the presence of TBAH in the final product, elemental C, H, and N analyses were not performed. The IR spectrum reveals the presence of uncoordinated nitrate as well as of PF_6^-. As for **1**, the presence of a Cu–Cl stretching vibration was not detected in the IR spectrum. Cluster **5** was further characterized by ICP analysis (Pt:Au:Cu = 1:6.2:1.1), ^{31}P NMR, ^{195}Pt NMR, and ^1H NMR spectroscopy and by means of FAB-MS.

The ^{31}P NMR spectrum of **5** shows there is one phosphine bonded directly to the platinum atom, which is in central position surrounded by six $AuPPh_3$ units. This is also in agreement with the 1:6 intensity ratio of septet:doublet. The $AuPPh_3$ units give rise to one resonance, thereby pointing to a fluxional behaviour of these phosphine sites in solution. The appearance of the ^{31}P NMR spectrum is identical to that of $[Pt(H)(PPh_3)(AuX)(AuPPh_3)_6]^+$ (X = Cl, Br, I).[49] The $^{195}Pt\{^1H\}$ NMR spectrum (Figure 4A) also shows the presence of one phosphine ligand bonded directly to Pt and of six $AuPPh_3$ units.

The ^1H-coupled ^{195}Pt NMR spectrum of **5** (Figure 4B) shows an additional doublet splitting due to $^1J(Pt-^1H) = 606$ Hz. This coupling is similar to that found in other hydride-containing PtAu clusters[9,10,17,28,29] and is even identical to that in $[Pt(H)(PPh_3)(AuI)(AuPPh_3)_6]^+$,[49] and therefore indicates the presence of a hydride ligand bonded directly to the central platinum atom. The ^1H NMR resonance for **5** is located at $\delta = +0.46$ ppm, considerably shifted downfield as compared to terminal platinum hydrides.[35,47] Together with the magnitude of $^1J(H-^{195}Pt) =$ 606 Hz and the absence of a terminal Pt–H stretching vibration in the IR spectrum, this is taken as strong evidence for the bridging position of the hydride ligand between the central platinum and peripheral metal (gold, vide infra) atoms.

Considerations on Molecular Structure. The molecular geometry of **5** as a solid is supposed to resemble that of the isoelectronic parent $[Pt(H)(PPh_3)(AuPPh_3)_7]^{2+}$ cluster,[17] which also is a spheroidal $(S^\sigma)^2(P^\sigma)^6$ $Pt(H)(P)(M)_7$ cluster. This structure is derived from a cubic geometry, with Pt in central position surrounded by seven metal atoms at the vertices of a cube; the platinum bonded phosphine ligand is situated at the remaining eighth vertex. It is then interesting to speculate on the three possible isomers for **5**, arising from different positions for the CuCl unit (Figure 5). From the metal positions in these figures it is evident that for all three isomers the bridging hydride ligand is located at the "open" side. It is then postulated, in analogy with the observed structures of **1** and **2**, that isomer A corresponds to the most stabilized geometry, because in this arrangement the relatively electronegative H ligand is situated "trans" to the copper, which is less electronegative than gold.

The molecular composition of **5** was also confirmed by positive ion FAB-MS, which has been proved to be a successful technique for the determination of the molecular composition of cationic clusters.[12] The positive ion FAB-MS in the 2200–3500 mass range has a large number of peaks of which a

(49) Schoondergang, M. F. J.; Bour, J. J.; van Strijdonck, G. P. F.; Schlebos, P. P. J.; Bosman, W. P.; Smits, J. M. M.; Beurskens, P. T.; Steggerda, J. J. *Inorg. Chem.* **1991**, *30*, 2048.
(50) Vollenbroek, F. A.; Bour, J. J.; van der Velden, J. W. A. *Recl. Trav. Chim. Pays-Bas* **1980**, *99*, 137.
(51) Vollenbroek, F. A. Syntheses and Investigations of Gold Cluster Compounds. Thesis, University of Nijmegen, Nijmegen, 1979.
(52) Cariati, F.; Naldini, L. *Inorg. Chim. Acta* **1971**, *5*, 172.

selection of the centroids as well as their assignment is given in Table 7. No significant peaks with masses higher than that of M^+ are observed. This FAB-MS result is, like all other previously described data, in agreement with the formulation of **5** as $[Pt(H)(PPh_3)(CuCl)(AuPPh_3)_6]^+$.

In this paper several hydride containing mixed-metal−gold phosphine clusters have been reported. It was show that in $[Pt(H)(AuPy)(AuPPh_3)_8](NO_3)_2$ (**3**) a pyridine ligand is bonded to a gold atom and that this pyridine ligand can be replaced by Cl^-, Br^-, and SCN^- to yield the related compounds **4a**, **4b**, and **4c** respectively. In addition to these pure PtAu clusters, three copper-containing hydride clusters were characterized. The crystal structures of $[Pt(H)(CuCl)(AuPPh_3)_8](NO_3)$ (**1**) and $[Pt(H)(CuCl)_2(AuPPh_3)_8](NO_3)$ (**2**) show that the copper atoms are located "trans" to the hydride ligand and that in **2** the copper atoms are not in neighboring positions with respect to each other.

Acknowledgment. This investigation was supported by the Netherlands Foundation for Chemical Research (SON) with fundamental support from the Netherlands Organization for the Advancement of Pure Research (NWO). We gratefully thank Mrs. Nicole P. W. Langenhuizen, Mr. Reinout J. N. A. M. Kicken and Mr. Marcel E. van der Woude for their contributions as part of their undergraduate research. We also acknowledge Prof. L. H. Pignolet for his fruitful discussions and for providing us the opportunity to do FAB-MS experiments.

Supplementary Material Available: Tables of crystallographic details and additional fractional positional parameters, anisotropic thermal parameters, and bond distances and angles (42 pages). Ordering information is given on any current masthead page.

IC941008A